

# Infinite Ergodic Theory for Heterogeneous Diffusion Processes

N. Leibovich and E. Barkai

*Department of Physics, Institute of Nanotechnology and Advanced Materials, Bar-Ilan University, Ramat-Gan 5290002, Israel*

We show the relation between processes which are modeled by a Langevin equation with multiplicative noise and infinite ergodic theory. We concentrate on a spatially dependent diffusion coefficient that behaves as  $D(x) \sim |x - \tilde{x}|^{2-2/\alpha}$  in the vicinity of a point  $\tilde{x}$ , where  $\alpha$  can be either positive or negative. We find that a nonnormalized state, also called an infinite density, describes statistical properties of the system. For processes under investigation, the time averages of a wide class of observables, are obtained using an ensemble average with respect to the nonnormalized density. A Langevin equation which involves multiplicative noise may take different interpretation; Itô, Stratonovich, or Hänggi-Klimontovich, so the existence of an infinite density, and the density's shape, are both related to the considered interpretation and the structure of  $D(x)$ .

PACS numbers:

## I. INTRODUCTION

Consider a signal  $x(t)$  which is modeled with a Langevin equation

$$\frac{dx}{dt} = \sqrt{D(x)}\eta(t), \quad (1)$$

where  $D(x)$  is spatially dependent and  $\eta(t)$  is a white noise with zero mean and  $\langle \eta(t+t')\eta(t) \rangle = \delta(t')$ . The initial condition is  $x(t)|_{t=0} = x_0$ . This is a model for diffusion of a particle in an inhomogeneous system, where  $x(t)$  is the trajectory of the particle. Such spatially dependent diffusivities model many processes, where a partial list includes random walks in an inhomogeneous medium [1–3], chemical reactions [4], diffusion (in momentum space) in laser cooling processes [5, 6], dissipative particle dynamics [7], vortex-antivortex annihilations [8], studies of the stocks market in finances [9], in biophysics [10–12] e.g. measurements of proteins' diffusivity in mammalian cells [12], and modeling of  $1/f^\beta$  noise [13].

Importantly, care must be taken when dealing with multiplicative noise, since the Langevin equation may take different interpretations; Itô, Stratonovich or Hänggi-Klimontovich (isothermal) [4, 14–18], see also Table I. Generally, the interpretation of integration is related to the examined process and the nature of the noise [4, 18–20]. The corresponding Fokker-Planck equation reads

$$\frac{\partial P(x,t)}{\partial t} = \frac{1}{2} \frac{\partial}{\partial x} \left\{ D(x)^{1-\frac{A}{2}} \frac{\partial}{\partial x} \left[ D(x)^{\frac{A}{2}} P(x,t) \right] \right\}, \quad (2)$$

with  $A = 0$  for Hänggi-Klimontovich,  $A = 1$  for Stratonovich, or  $A = 2$  for Itô interpretation. Clearly, the solution of the Fokker-Planck equation,  $P(x,t)$ , depends on the behavior of  $D(x)$  and the interpretation of Eq. (1).

In the long time limit, a system may reach a steady state, namely  $P(x,t)$  for long  $t$  is time independent. This solution is usually reached from most typical initial conditions, and the time-independent density is called the invariant density [21]. For example when Brownian particles are confined in a finite domain, after a sufficiently

long time their concentration becomes uniform (for reflecting boundary conditions) and thus time invariant. Ergodic theory studies the properties of invariant densities. For dynamical systems, Birkhoff's ergodic theorem states that if such an invariant density exists (i.e. it is normalizable) the ergodic assumption is fulfilled, namely the time-averaged observable converges to the average with respect to the normalized invariant measure [21]. However, in some cases such an invariant state is nonnormalizable, and thus does not serve as a proper density. When the so-called infinite invariant density is found, a different type of ergodic framework emerges, and this is called infinite ergodic theory. The mathematical concept of infinite densities was thoroughly investigated [22, 23].

As was mentioned, the term “infinite density” refers to a function which is nonnormalizable. Still, as we show below, this nonnormalizable state can describe statistical properties of the process. At first glance this seems like a contradiction since, as mentioned, a proper density is normalizable. Nevertheless, the infinite density captures some information on certain observables. Our work is inspired by infinite ergodic theory which addresses deterministic paths, like the Pomeau-Maneville map [24, 25]. The concept was extended also to models of laser-cooled atoms, Lévy walks, and non-equilibrium processes [26–28]. The statistical properties of observables that are integrable with respect to the invariant density are given by Aaronson-Darling-Kac theorem [29, 30].

In this paper, we demonstrate some features of infinite ergodic theory using a process which is modeled by a Langevin equation with multiplicative noise. In particular, we examine the heterogeneous diffusion model with a power-law dependent diffusion coefficient in the vicinity of some point  $\tilde{x}$ , i.e.

$$D(x) \propto |x - \tilde{x}|^{2-2/\alpha}. \quad (3)$$

This, for example, is related to Richardson diffusion in turbulence [31], or generalized Lotka-Volterra equations modeling ecosystems [32].  $\alpha = 1$  is the “normal” case, where  $D$  is simply a constant. It was shown that such processes yield anomalous diffusion, and the distribution of time-averaged mean-squared displacement was also

Model [Ref.]	Form	$D(x)$	Comments
Vortex-Antivortex Annihilation [8]	S	$\propto 1/\ln x$	
1/f Noise [13]	I	$\propto x^{2\eta}$	
Nonlinear systems satisfying Einstein relation [17]	HK	$\propto 1 + Bx^a$	
Atmospheric Diffusion [31]			$\partial_t P = \epsilon \partial_x [x^{4/3} \partial_x P]^b$
Ecosystems [32]	I	$\propto x$	
Diffusion on a Fractal [37, 38]			$\partial_t P = K x^{1-D} \partial_x [x^{-1-\theta+D} \partial_x P]^c$

<sup>a</sup>This is given for Van der Pol oscillators.  $B$  is a constant proportional to the temperature.

<sup>b</sup> $\epsilon$  is a constant.

<sup>c</sup> $K$  is a constant,  $D$  is the fractal dimension.  $\theta$  is related to the anomalous diffusion exponent.

TABLE I: Examples of models which have spatially dependent  $D(x)$ , with different interpretations of the Langevin equation (1); Itô (I), Stratonovich (S), or Hänggi-Klimontovich (HK). For some models, a form of a Langevin equation (1) is not given, though an equation for the PDF  $P(x, t)$  is provided, see [31, 37, 38].

considered, so it is known that standard ergodic theory does not hold here [33–36]. The question is thus what is the proper ergodic theory for these anomalous processes? Here we show that the basic aspects mentioned above; a limit state which is nonnormalizable, infinite ergodic theory, and the Aaronson-Darling-Kac theorem are applicable for this model as well.

## II. FROM MULTIPLICATIVE NOISE TO BESSEL PROCESS

In [8], Bray shows that a specific model of vortex-antivortex annihilation, which involves multiplicative noise, is closely related to the motion of a random walker in a central logarithmic potential, namely a Bessel process. Here we extend this result and show that processes with  $D(x)$  in the form of Eq. (4) (see below) are associated with the Bessel process as well.

Consider the Langevin equation (1) with

$$\sqrt{D(x)} = \sqrt{2D_0\alpha^2} \left(\frac{x}{\ell}\right)^{1-\frac{1}{\alpha}}. \quad (4)$$

The constant  $D_0$  has units of  $[\text{cm}^2\text{sec}^{-1}]$ , and  $\ell$  is some characteristic length scale. Generally the exponent  $\alpha$  may be positive or negative. Currently, we concentrate on the case where  $\alpha \geq 1$  and  $x \in [0, \infty)$ , so the growth condition is fulfilled (see [4] and App. A), thus we ensure stability of the paths. We also require  $(1-A)(1-\alpha) < 1$  for a reason that we will clarify soon. Initially, all particles are located in  $x(t)|_{t=0} = x_0$ . At  $x = 0$  we use

a reflecting boundary condition. The specific choice in Eq. (4) allows an exact treatment of the problem for any time  $t$ . Later we consider a more general form of the diffusion field.

There is a known mapping between Itô and Hänggi-Klimontovich forms of Eq. (2) to Stratonovich interpretation (see e.g. [17] and App. B). The Fokker-Planck equation (2) is rewritten

$$\begin{aligned} \frac{\partial P(x, t)}{\partial t} = & \frac{1}{2} \frac{\partial}{\partial x} \left[ \sqrt{D(x)} \frac{\partial}{\partial x} \sqrt{D(x)} P(x, t) \right] \\ & - \frac{1-A}{2} \frac{\partial}{\partial x} \left[ \sqrt{D(x)} \frac{\partial \sqrt{D(x)}}{\partial x} P(x, t) \right]. \end{aligned} \quad (5)$$

Thus, the Stratonovich interpretation of a Langevin equation with an additional effective drift term (i.e. the second term on the right-hand side in Eq. (5)) is equivalent to the Langevin equation (1) with the Hänggi-Klimontovich ( $A = 0$ ) or Itô ( $A = 2$ ) forms. Its corresponding Langevin equation is

$$\frac{dx}{dt} = \sqrt{D(x)}\eta(t) + \frac{1-A}{2} \sqrt{D(x)} \frac{d\sqrt{D(x)}}{dx}, \quad (6)$$

which is now interpreted via the Stratonovich approach.

Now we define the transformation [8, 33]

$$y(x) \equiv \int_0^x \frac{dx}{\sqrt{D(x)}} = \frac{\ell^{1-\frac{1}{\alpha}}}{\sqrt{2D_0}} x^{\frac{1}{\alpha}} \quad (7)$$

where  $y \in [0, \infty)$  and  $y_0 \equiv y(x_0)$ . The above transformation may be used only when interpreting the noise as continuous, namely in the Stratonovich form (i.e. following Wong-Zakai theorem [19]). Therefore we obtain that Eq. (6) is mapped to

$$\dot{y} = \eta(t) + \frac{1-A}{2} \cdot \frac{d\sqrt{D(y)}}{dy} \frac{1}{\sqrt{D(y)}}, \quad (8)$$

then, using Eqs. (4) and (7) we find

$$\dot{y} = \eta(t) - \frac{U_0/2}{y}, \quad (9)$$

where  $U_0 = (1-A)(1-\alpha)$ . The variable  $y$  describes the position of a Brownian particle in a logarithmic potential so the additional effective force is given by  $F(y) = -\frac{1}{2}U_0/y = -\frac{1}{2}U_0\partial_y \ln y$ . Note that the potential can be repulsive or attractive. Eq. (9) is the Bessel process which is related to the diffusion of particles in high dimension, where  $y$  is the radial displacement, and  $U_0$  is associated with the dimension [8, 39]. The probability density function (PDF) of  $y$  in time  $t$ , with the initial condition  $P(y, t)|_{t=0} = \delta(y-y_0)$ , and the reflecting boundary condition, i.e.  $\partial_y P(y, t)|_{y=0} = 0$ , is

$$P(y, t; y_0, 0) = e^{-\frac{y^2+y_0^2}{2t}} y^{\frac{1}{2}+\frac{U_0}{2}} y_0^{\frac{1}{2}-\frac{U_0}{2}} I_{-\frac{1}{2}-\frac{U_0}{2}} \left( \frac{y_0 y}{t} \right) \frac{1}{t}, \quad (10)$$

where  $I_\nu(z)$  refers to the modified Bessel function of the first kind of order  $\nu$  [8, 39]. This PDF is normalized when  $U_0 < 1$ , so here  $(1-A)(1-\alpha) < 1$  as mentioned. Back to  $P(x, t)$  using Eq. (7) we find that

$$P(x, t) = \mathcal{N} \exp \left[ -\frac{(x^{\frac{2}{\alpha}} + x_0^{\frac{2}{\alpha}}) \ell^{2-\frac{2}{\alpha}}}{4D_0 t} \right] \quad (11)$$

$$x_0^{\frac{1}{2\alpha}(1+U_0)} x^{\frac{1}{2\alpha}(3-U_0-2\alpha)} I_{-\frac{1}{2}-\frac{U_0}{2}} \left( \frac{x_0^{\frac{1}{\alpha}} x^{\frac{1}{\alpha}} \ell^{2-\frac{2}{\alpha}}}{2D_0 t} \right) \frac{1}{t}$$

where  $\mathcal{N} = \ell^{2-\frac{2}{\alpha}}/[2D_0\alpha]$  is the normalization constant. It is easy to verify that Eq. (11) is the normalized solution of Eq. (2), with the initial condition  $P(x, 0) = \delta(x - x_0)$ . We note that the following results are also valid for sufficiently long time for other initial concentrations which are inherently narrow, e.g. Gaussian distribution centered in  $x_0$ .

**Comment:** Mathematically, the above solution, Eq. (11), exists when  $U_0 \equiv (1-A)(1-\alpha) < 1$ . For stronger effective potential, when  $U_0 \geq 1$ , the particles fall to the origin, thus the only solution is when zero serves as an absorbing point, see discussion in [8]. A regularization of the diffusion at the vicinity of the origin settles the problem with  $U_0 \geq 1$ , as commented in [8] and we show below in Sec. IID.

We will soon relax the conditions made in this section. The requirements  $U_0 < 1$  with  $\alpha \geq 1$ , limit the range of  $\alpha$  for Itô interpretation, so here  $1 \leq \alpha < 2$  for  $A = 2$ . For Hänggi-Klimontovich ( $A = 0$ ) and Stratonovich ( $A = 1$ ) interpretations we use  $\alpha \geq 1$ . Moreover we note that our results are valid for finite  $\alpha$  only, where essentially different results are obtained in the limit  $\alpha \rightarrow \infty$ . This case, where  $D(x) \propto x^2$ , is not of the scope of this paper and is excluded.

### A. Infinite Density

To gain insight on the long-time limit of the solution we write Eq. (2) as  $\partial_t P = -\partial_x J$ , where

$$J \equiv -\frac{1}{2} D(x)^{1-\frac{A}{2}} \partial_x \left[ D(x)^{\frac{A}{2}} P(x, t) \right]. \quad (12)$$

In many circumstances, when setting  $J = 0$  the steady-state solution  $P(x, t) = P_{ss}(x)$ , which is an invariant density, is obtained. In our case, there is no steady state in the usual sense, but still we search for a solution  $\mathcal{I}_\infty(x)$  that satisfies

$$D(x)^{1-\frac{A}{2}} \partial_x \left[ D(x)^{\frac{A}{2}} \mathcal{I}_\infty(x) \right] = 0, \quad (13)$$

which is an infinite density. Here, the solution of zero current,  $J = 0$ , obtained from Eq. (13), is

$$\mathcal{I}_\infty(x) = C D(x)^{-\frac{A}{2}} = C \frac{1}{(2D_0\alpha^2)^{A/2}} \left( \frac{x}{\ell} \right)^{A(-1+\frac{1}{\alpha})}. \quad (14)$$

While solving  $\partial_t P = 0$  one finds another solution which diverges when  $x$  goes to infinity, hence cannot capture a physical sense, thus the only solution is given when  $J = 0$ . However, the solution Eq. (14), is not normalizable, hence as a stand alone solution it is not valid. Therefore, the constant  $C$  is not related to the normalization in the usual way. Note that since  $U_0 < 1$  and  $\alpha \geq 1$  [equivalent to  $-1 < A(-1+1/\alpha) \leq 0$ ] the divergence in the spatial integral  $\int_0^\infty dx \mathcal{I}_\infty(x)$  is caused by the large  $x$  behavior of  $\mathcal{I}_\infty(x)$ . Importantly, note that there is a relation between the nonnormalizable zero-current solution Eq. (14) and the time-dependent distribution Eq. (11) via

$$\lim_{t \rightarrow \infty} P(x, t) t^{\frac{\alpha}{2} - \frac{A}{2}(\alpha-1)} = \mathcal{I}_\infty(x)$$

$$= C \frac{1}{(2D_0\alpha^2)^{A/2}} \left( \frac{x}{\ell} \right)^{A(-1+\frac{1}{\alpha})}, \quad (15)$$

where  $C = 2^{1-\alpha(1-A)-\frac{A}{2}} D_0^{-\frac{\alpha(1-A)}{2}} \ell^{-U_0} |\alpha|^{A-1} / \Gamma \left[ \frac{1-U_0}{2} \right]$ . This solution is called an infinite density in the sense that it is nonnormalizable. From Eq. (15) it is easy to understand why  $\mathcal{I}_\infty(x)$  is not normalized. On the left-hand side we have  $P(x, t)$  times a prefactor that increases with time. Since the area under  $P(x, t)$  is unity, but  $t^{(\alpha-A\alpha+1)/2} \rightarrow \infty$ , clearly the integral over  $\mathcal{I}_\infty$  must blow up. More surprising is that this nonnormalized state captures some of the physical properties of the process as is shown below.

### B. Infinite Ergodic Theory

Consider an observable  $\mathcal{O}[x(t)]$ , which depends on the realization  $x(t)$ . Assume that the observable  $\mathcal{O}[x(t)]$  fulfills the following requirement

$$\int_0^\infty dx \mathcal{O}[x] \mathcal{I}_\infty(x) < \infty, \quad (16)$$

namely the observable is integrable with respect to  $\mathcal{I}_\infty(x)$ . The time average of  $\mathcal{O}[x(t)]$  is defined as

$$\overline{\mathcal{O}}_t \equiv \frac{1}{t} \int_0^t dt' \mathcal{O}[x(t')], \quad (17)$$

and the ensemble average reads

$$\langle \mathcal{O}_t \rangle \equiv \int_0^\infty dx \mathcal{O}[x] P(x, t). \quad (18)$$

Generally both  $\overline{\mathcal{O}}_t$  and  $\langle \mathcal{O} \rangle$  are time dependent. In the long time limit, using Eq. (15), we obtain

$$\langle \mathcal{O}_t \rangle \stackrel{t \rightarrow \infty}{\approx} t^{\beta-1} \int_0^\infty dx \mathcal{O}[x] \mathcal{I}_\infty(x), \quad (19)$$

with

$$\beta = 1 - \frac{\alpha}{2} - \frac{A}{2}(1-\alpha) = \frac{1}{2} + \frac{U_0}{2}. \quad (20)$$

Now consider the ensemble average of the time average

$$\begin{aligned}\langle \overline{\mathcal{O}}_t \rangle &\equiv \int_0^\infty dx P(x, t) \frac{1}{t} \int_0^t dt' \mathcal{O}[x(t')] \\ &\equiv \frac{1}{t} \int_0^t dt' \int_0^\infty dx \mathcal{O}[x] P(x, t').\end{aligned}\quad (21)$$

Therefore we find

$$\begin{aligned}\langle \overline{\mathcal{O}}_t \rangle &\equiv \frac{1}{t} \int_0^t dt' \int_0^\infty dx \mathcal{O}[x] P(x, t') \\ &\stackrel{t \rightarrow \infty}{\approx} \frac{1}{t} \int_0^t dt' t'^{\beta-1} \int_0^\infty dx \mathcal{O}[x] \mathcal{I}_\infty(x) \\ &= \frac{t^{\beta-1}}{\beta} \int_0^\infty dx \mathcal{O}[x] \mathcal{I}_\infty(x),\end{aligned}\quad (22)$$

where the prefactor  $1/\beta$  [see Eq. (20)] comes from the time integration. Hence, using Eqs. (19) and (22), we conclude that

$$\lim_{t \rightarrow \infty} \frac{\beta \langle \overline{\mathcal{O}}_t \rangle}{\langle \mathcal{O}_t \rangle} = 1. \quad (23)$$

Thus, time and ensemble averages are related, and the limit  $\beta \rightarrow 1$  corresponds to the standard ergodic theory.

Furthermore,  $\overline{\mathcal{O}}_t$  is a stochastic variable determined by the trajectory of  $x(t)$  thus we define the random variable

$$\xi \equiv \lim_{t \rightarrow \infty} \frac{\beta \overline{\mathcal{O}}_t}{\langle \mathcal{O}_t \rangle}. \quad (24)$$

In the following we examine the PDF of  $\xi$  (clearly with  $\langle \xi \rangle = 1$ ), where  $0 < \beta < 1$  (i.e.  $-1 < U_0 < 1$ , weak potential).

For example let us consider the observable  $\mathcal{O}[x(t)] = \theta(0.4 < x(t) < 0.6)$  which is a pulse function. Thus  $\mathcal{O}[x(t)]$  alternates between  $\mathcal{O}[x(t)] = 1$  when  $x(t) \in (0.4, 0.6)$  and  $\mathcal{O}[x(t)] = 0$  otherwise. The time integration of the pulse function is the occupation time in the domain, so  $\overline{\mathcal{O}}_t$  is the time spent by the process in the interval  $(0.4, 0.6)$  divided by the measurement time. Using [8, 39, 40] we deduce that the sojourn times (i.e. first passage time) PDF when  $\mathcal{O}[x(t)] = 0$  (i.e. outside the interval) follows

$$\psi(\tau) \sim \tau^{-1-\beta}, \quad (25)$$

in the long time limit (see [8, 39, 40] and App. C). Here the average sojourn time of the particle beyond the observation domain [outside the interval  $(0.4, 0.6)$ ] diverges  $\langle \tau \rangle = \infty$  since  $0 < \beta < 1$ . The number of times  $x(t)$  re-enters the interval under observation until time  $t$  is  $n(t)$ ,  $\overline{\mathcal{O}}_t \propto n$  and since  $\langle \xi \rangle = 1$  (as mentioned) we have

$$\xi \equiv \beta \overline{\mathcal{O}}_t / \langle \mathcal{O} \rangle \sim n(t) / \langle n \rangle. \quad (26)$$

This equation means that the distribution of the normalized time-average is the same as the distribution of the

number of renewals. From the renewal processes studies we know that the number of renewals up to time  $t$  divided with its mean (i.e. the variable  $\xi$ ) is given by Mittag-Leffler distribution of order of  $\beta$ ,  $\mathcal{M}_\beta(\xi)$ , see e.g. [41, 42]. Therefore the distribution of  $\xi$  is expected to follow the Mittag-Leffler distribution as well, i.e.

$$P(\xi) = \mathcal{M}_\beta(\xi) \equiv \frac{\Gamma^{\frac{1}{\beta}}(1+\beta)}{\beta \xi^{1+\frac{1}{\beta}}} L_\beta \left[ \frac{\Gamma^{\frac{1}{\beta}}(1+\beta)}{\beta \xi^{\frac{1}{\beta}}} \right], \quad (27)$$

where  $L_\beta(z)$  is the one-sided Lévy density of order  $\beta$ , which is defined through the following inverse Laplace transform from  $s$  to  $z$ ;  $L_\beta(z) \equiv \mathcal{L}^{-1}[\exp(-s^\beta)]$ , see App. D. The above argument, Eq.(27), also applies to any observable which fulfills Eq. (16), namely where it is integrable with respect to an infinite measure of a system [30]. This result is in the spirit of the Aaronson-Darling-Kac theorem usually applied in the context of deterministic setting [29].

For some intuition of the results consider a free Brownian particle with realization  $y(t)$ . There, the sojourn times  $\tau$  of the trajectory  $y(t)$  outside a given finite interval are distributed with  $\psi(\tau) \sim \tau^{-3/2}$ . The transformation  $y(x)$  given in Eq. (8) is stretching or compressing the space in such a way that the temporal properties such as the return times behave similarly for  $y$  and  $x$ . Therefore, the sojourn times of the realization  $x(t)$  with Stratonovich interpretation (which is mapped into a free Brownian particle) outside a finite interval in  $x$  space, is  $\psi(\tau) \sim \tau^{-3/2}$ , namely  $\beta = 1/2$ . For Itô and Hänggi-Klimontovich interpretations the results, Eqs. (23) (27) with (20), are similar to the ones found in diffusion in Logarithmic potential [28]. Roughly speaking, now with the mapping to Bessel processes at our hand, we can apply these general results, to the case under study here: diffusion in inhomogeneous medium.

### C. Simulation Results

In Fig. 1 we demonstrate the long sojourn times close to zero. We generate a trajectory  $x(t)$  from the Langevin equation (1) with (4) and Stratonovich interpretation. We use  $\alpha = 3/2$  and the measurement time is  $10^4$ . In all simulations in this paper we use  $D_0 = 1/2$  and  $\ell = 1$ .  $x(t)$  is given in the panel (A). In panel (B) we present the observable  $\mathcal{O}[x(t)] = \theta(0.4 < x(t) < 0.6)$  where  $x(t)$  is the same realization given in (A). In panel (C) we show the mathematical observable  $\mathcal{O}[x(t)] = \sin[1/x(t)]$ , which is chosen to demonstrate the fact that the choice of a specific observable is not important. Both observables [in panels (B) and (C)] are integrable with respect to the infinite density. Therefore, they share a similar property; the observables have long sojourn times close to zero, thus Eq. (27) with  $\beta = 1/2$  in agreement with Eq. (20) is valid, see Fig. 1.

In Fig. 2 we present the simulation results of  $P(x, t)$  for processes  $\sqrt{D(x)} = \alpha x^{1-1/\alpha}$  where  $\alpha = 3/2$ . Panel

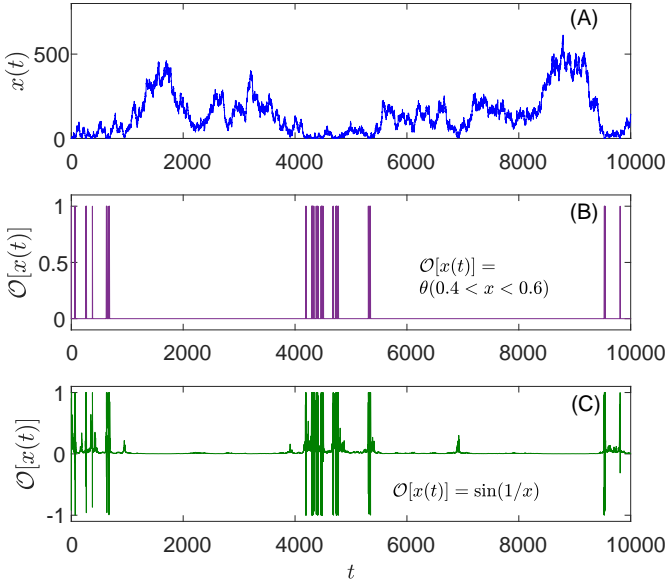


FIG. 1: A trajectory  $x(t)$  [panel (A)] and its corresponding observable  $\mathcal{O}[x(t)] = \theta(0.4 < x(t) < 0.6)$  [panel (B)] and  $\mathcal{O}[x(t)] = \sin[1/x(t)]$  [panel (C)]. The signal is generated from Langevin equation (1) with (4) and Stratonovich interpretation. Here we use  $\alpha = 3/2$  and the measurement time is  $10^4$ . The long sojourn times of  $\mathcal{O}[x(t)]$  close to zero are visible.

(A) presents the results for Hänggi-Klimontovich interpretation ( $A = 0$ ), panel (B) for Stratonovich ( $A = 1$ ), and (C) shows results for Itô interpretation ( $A = 2$ ). The agreement between the simulation results (symbols), the time-dependent solution Eq. (11) (solid lines) and the limit distribution Eq. (15) (dashed lines) is visible. These simulations clearly demonstrate that the nonnormalized state is measurable. Of-course for finite times we see deviations, however as we increase the measurement time, the nonnormalized state is approached.

As explained above, for an observable  $\mathcal{O}[x(t)]$  which is integrable with respect to  $\mathcal{I}_\infty(x)$  infinite ergodic theory holds. For the illustration we choose  $\mathcal{O}[x(t)] = \theta(0.4 < x(t) < 0.6)$  and define the random variable  $\xi$  using Eq. (24). Then, in the long time limit,  $P(\xi)$  follows the Mittag-Leffler distribution of order  $\beta$ . In Fig. 3 we present the simulation results (with symbols) for the PDF of  $\xi$  where  $\alpha = 1.4$ ,  $t = 10^3$  and  $10^5$  particles. Panel (A) presents results for Hänggi-Klimontovich (Mittag-Leffler function of order 0.3), panel (B) presents the results for Stratonovich (Mittag-Leffler of order 0.5) and (C) for Itô interpretation (Mittag-Leffler of order 0.7). Here we demonstrate that the statistics of  $\xi$  depends on the stochastic interpretation of the Langevin equation (1).

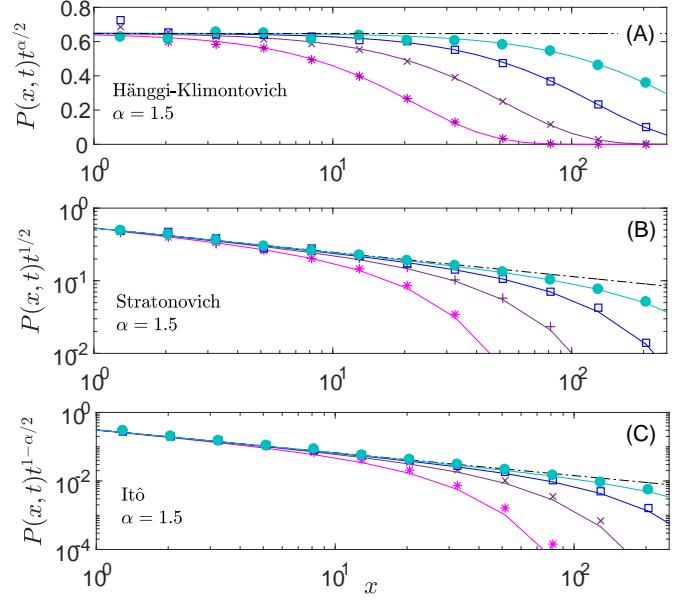


FIG. 2: The scaled PDF  $t^{1-\beta} P(x, t)$  for different times with  $\sqrt{D(x)} = \alpha x^{-1/\alpha}$  where  $\alpha = 3/2$  and  $x > 0$ . Panel (A) presents the results for Hänggi-Klimontovich interpretation, panel (B) for Stratonovich interpretation and panel (C) shows the results for the Itô interpretation. Here we present the simulation results for  $t = 31$  (pink stars),  $t = 100$  (purple crosses),  $t = 316$  (blue squares) and  $t = 1000$  (cyan full circles). The number of particles is  $10^5$ . Note that the upper panel is presented in semi-log scale while the other panels are given in double-log scale. An agreement between simulation results (symbols), the analytical prediction Eq. (11) (solid lines), and the limit behavior Eq. (15) (dashed line) is shown. In the long limit the nonnormalized state  $\mathcal{I}_\infty(x)$  is approached, even though  $P(x, t)$  is normalized for any finite time.

#### D. Other Structures of $D(x)$

As was mentioned in the Introduction, we study processes where, in the vicinity of some point  $\tilde{x}$ , the diffusion coefficient is Eq. (3). In the previous subsections we considered a specific form of  $D(x)$ , Eq. (4), which allowed us to obtain exact results for any time  $t$ . Our aim now is to show that the features such as the infinite density are generally valid, in particular for processes with  $D(x) \neq 0$  on  $x = 0$ . For example consider a process with

$$\sqrt{D(x)} = \sqrt{2D_0} \cdot \begin{cases} 1 & |x| < x_c \\ \alpha \left| \frac{x}{\ell} \right|^{1-1/\alpha} & |x| \geq x_c \end{cases} \quad (28)$$

where  $x_c = \ell \alpha^{\frac{\alpha}{1-\alpha}}$ , so  $D(x)$  is continuous. We define the process in  $(-\infty, \infty)$ . Furthermore, to fulfill the growth condition we demand  $\alpha > 0$ , see [4] and App. A. Here,

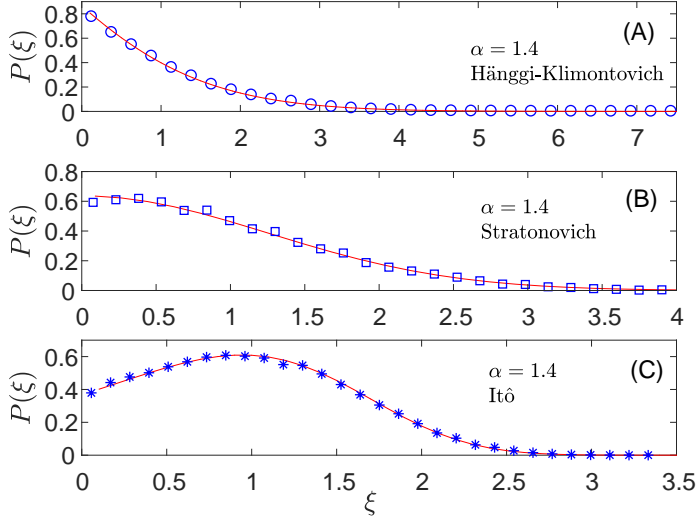


FIG. 3: The distribution of the random variable  $\xi$  defined in Eq. (24) with  $\mathcal{O}[x(t)] = \theta(0.4 < x(t) < 0.6)$  and  $D(x)$  is given in Eq. (4) with  $\alpha = 1.4$ . The simulation results are presented in blue circles [panel (A), Hänggi-Klimontovich], blue rectangles [panel (B), Stratonovich] and blue stars [panel (C), Itô]. For the simulation we use  $10^5$  particles,  $\alpha = 1.4$  and  $t = 10^3$ . The red curves represent the analytic predictions; Mittag-Leffler of order  $\beta = 0.3$  (A),  $0.5$  (B), and  $0.7$  (C), see Eq. (27)

using the transformation  $y(x) \equiv \int_0^x dx' D(x')^{-1/2}$ , we find

$$\frac{d\sqrt{D(y)}}{dy} \frac{1}{\sqrt{D(y)}} = \begin{cases} 0 & |y| < y_c \\ -\frac{U_0}{|y|} & |y| > y_c, \end{cases} \quad (29)$$

which is the effective force defined in Eq. (8). The concentration of Brownian particles with the effective force Eq. (29), initially on the origin and  $-1 < U_0 < 1$ , is

$$P(y, t) \approx \begin{cases} \frac{1}{\Gamma(\frac{1}{2} - \frac{U_0}{2})} |y|^{-U_0} (2t)^{\frac{U_0}{2} - \frac{1}{2}} e^{-\frac{y^2}{2t}} & |y| > y_c \\ \frac{1}{\Gamma(\frac{1}{2} - \frac{U_0}{2})} (y_c)^{-U_0} (2t)^{\frac{U_0}{2} - \frac{1}{2}} & |y| < y_c, \end{cases} \quad (30)$$

when the long-time limit is taken, see derivation in [43]. Back to  $P(x, t)$  we obtain

$$P(x, t) \approx \frac{1}{\Gamma[\frac{1-U_0}{2}]} \frac{\ell^{-U_0 + \frac{U_0}{\alpha}}}{(4D_0 t)^{(1-U_0)/2}} \cdot \begin{cases} \frac{1}{\alpha} \left| \frac{x}{\ell} \right|^{-1+\frac{1}{\alpha}} |x|^{-\frac{U_0}{\alpha}} \exp\left[-\frac{\ell^2 - \frac{2}{\alpha} x \frac{2}{\alpha}}{4D_0 t}\right], & |x| \geq x_c, \\ x_c^{-\frac{U_0}{\alpha}}, & |x| < x_c. \end{cases} \quad (31)$$

The infinite density, given by the condition  $J = 0$ , is

$$\mathcal{I}_\infty(x) = CD(x)^{-\frac{A}{2}} = \frac{C}{(2D_0)^{A/2}} \begin{cases} |\alpha|^{-A} \left| \frac{x}{\ell} \right|^{A(-1+\frac{1}{\alpha})}, & |x| \geq x_c, \\ 1, & |x| < x_c \end{cases} \quad (32)$$

so the relation

$$\lim_{t \rightarrow \infty} P(x, t) t^{\frac{\alpha}{2} - \frac{A}{2}(\alpha-1)} = \mathcal{I}_\infty(x), \quad (33)$$

holds, similarly to Eq. (15), with  $C = 2^{-\alpha(1-A) - \frac{A}{2}} D_0^{-\alpha(1-A)/2} \ell^{-U_0} |\alpha|^{A-1} / \Gamma[\frac{1-U_0}{2}]$ . As was mentioned above, from the existence of a nonnormalizable solution  $\mathcal{I}_\infty(x)$  related to  $P(x, t)$ , as given in (33), one can prove that Eqs. (23) and (27) with  $\beta$  given in Eq. (20) still hold, so infinite ergodic theory is valid. The proof and the results are similar to Sec. II B. From Eq. (32) we see that the nonnormalized state has a structure, which deviates from a pure power law Eq. (14). Generally, since  $\mathcal{I}_\infty(x) \propto D(x)^{-A/2}$ , the infinite density is specific to the details of the system.

## E. Ergodic Phase

In Eq. (28) we have regularized  $D(x)$  in the vicinity of the origin [compare with Eq. (4)], namely  $D(x) \neq 0$  when  $x \rightarrow 0$ . Therefore, when  $U_0 > 1$ , one finds a normalizable steady state and the process is ergodic, see [8, 43]. The equilibrium distribution is given by

$$P_{\text{eq}}(x) = \frac{1 - U_0}{2x_c(1 - U_0 - \alpha)} \begin{cases} |\alpha|^{-A} \left| \frac{x}{\ell} \right|^{A(-1+\frac{1}{\alpha})}, & |x| \geq x_c, \\ 1, & |x| < x_c \end{cases} \quad (34)$$

which is now normalized as usual, i.e.  $\int_{-\infty}^{\infty} P_{\text{eq}}(x) dx = 1$ , and the standard ergodic theory holds. It means that in the long time limit, when  $\mathcal{O}[x(t)]$  is integrable with respect to the equilibrium state, one finds

$$P(\xi) = \delta(\xi - 1), \quad (35)$$

where here  $\xi \equiv \lim_{t \rightarrow \infty} \overline{\mathcal{O}} / \langle \mathcal{O} \rangle$ . Interestingly, this ergodic phase is obtained when using Itô interpretation with  $\alpha > 2$ . For other forms (i.e. Stratonovich or Hänggi-Klimontovich) with  $\alpha > 0$  the ergodic phase cannot be obtained with Eq. (1). Needless to say that in this case, when adding a binding force to the Langevin equation (1), e.g. an harmonic potential, one may obtain an ergodic phase, with all interpretations.

## F. Simulation results

### 1. Scaled Time-Dependent Solution Approaches the Infinite Density - Stratonovich

Consider the Langevin equation (1) with the spatially dependent diffusion coefficient Eq. (28) with  $\alpha = 3/2$  and the initial position of all particles is on the origin, i.e.  $P(x, t)|_{t=0} = \delta(x)$ . In our simulations of the concentration we use the Langevin equation with Stratonovich interpretation. Here  $\beta = 1/2$  (see definition in Eq. (20)). In Fig. 4 we present  $P(x, t)t^{1/2}$  versus  $x$  for several times.

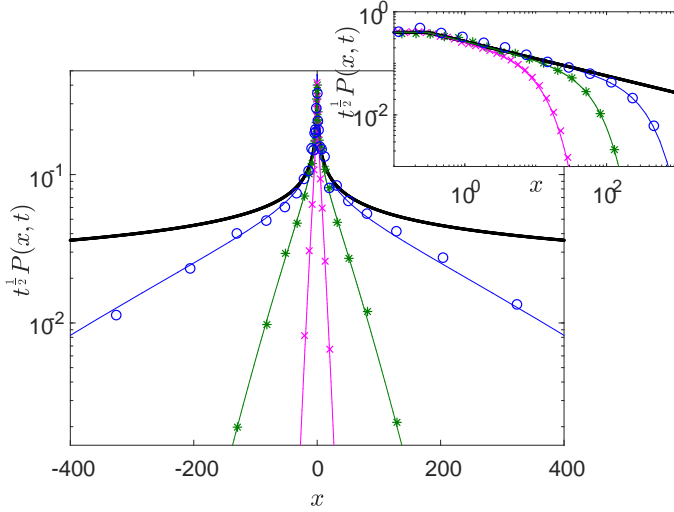


FIG. 4: The scaled concentration  $P(x, t)t^{1/2}$ , where  $D(x)$  is given in Eq. (28) with  $\alpha = 3/2$ , at times;  $t = 10$  (pink crosses),  $t = 10^2$  (green stars), and  $t = 10^3$  (blue circles). The colored lines and the black line represent the analytic expressions  $P(x, t)$  [Eq. (31)] and  $\mathcal{I}_{\infty}(x)$  [Eq. (32)], respectively. Inset: the data is presented in double-log scale, so the collapses at small  $x$  and the deviations from  $\mathcal{I}_{\infty}$  at large  $x$  are visible (only positive  $x$  is presented). For ensemble averaging we use  $10^4$  realizations.

The data collapse on a single curve is found for small  $x$  since then it merges with  $\mathcal{I}_{\infty}(x)$  which is a time-independent state.

## 2. Infinite Ergodic Theory and Ergodic Phase

We consider the observable  $\mathcal{O}[x(t)] = \theta(|x(t)| < x^*)$ , which means that  $\mathcal{O}[x(t)]$  is the indicator function. We investigate the random variable  $\xi$  Eq. (24). With the Stratonovich interpretation we expect

$$P(\xi) = \mathcal{M}_{1/2}(\xi) \equiv \frac{2}{\pi} \exp\left(-\frac{\xi^2}{\pi}\right), \quad (36)$$

i.e. the Mittag-Leffler distribution of order  $1/2$  which is one-sided Gaussian where clearly  $\langle \xi \rangle = 1$ . In the simulation results presented in Fig. 5 we choose  $\alpha = 3/2$  and  $x^* = 10$ . We compare between  $\langle \overline{\mathcal{O}}_t \rangle$  from the simulation and the analytic prediction  $2t^{1/2}/\langle \mathcal{O} \rangle \approx 7.17$ . To be precise we show that  $\langle \xi \rangle \rightarrow 1$  in the long time limit. Furthermore, we show that the distribution of  $\xi$  follows the one-sided Gaussian distribution Eq. (36) as expected, also for finite time simulations.

In addition, in Fig. 6 we present the simulation results, with  $\sqrt{D(x)}$  given by Eq. (28) and  $\alpha = 2$ . Then, the PDFs of  $\xi$ , presented with solid curves, are

$$P(\xi)_{\alpha \rightarrow 2} = \begin{cases} \exp(-\xi), & \text{HK,} \\ \frac{2}{\pi} \exp\left(-\frac{\xi^2}{\pi}\right), & \text{S,} \\ \delta(\xi - 1), & \text{I.} \end{cases} \quad (37)$$

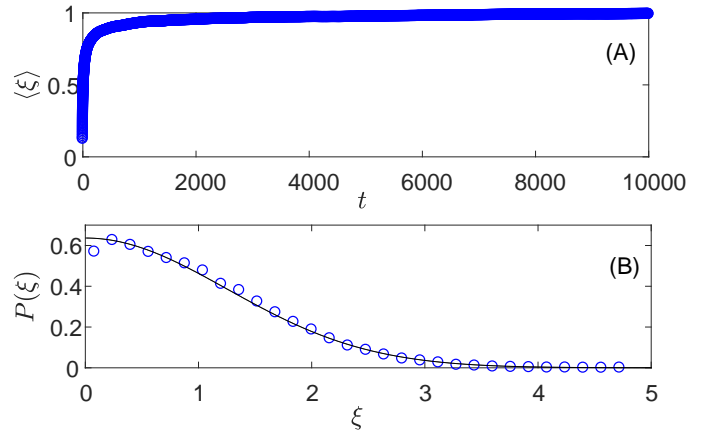


FIG. 5: Simulation of  $\xi$  defined in Eq. (24) with  $\mathcal{O}[x(t)] = \theta(|x(t)| < 10)$  and  $D(x)$  is given in Eq. (28). Panel (A): The convergence of  $\langle \xi \rangle$  to 1 in the long time limit. Panel (B): The distribution of the random variable  $\xi$ . The data from simulation is presented with open circles and the analytic curve Eq. (36) with a solid line. Here we use  $t = 10^4$ ,  $\alpha = 3/2$ , and  $5 \cdot 10^4$  realizations.

The derivation of these results is given in App. D. We compare these analytical results with the simulations when  $t = 10^5$ , and  $10^4$  particles. For the Itô interpretation the deviation from this analytic prediction, presented in Fig. 6 panel (C), is a finite time effect, since while increasing the measurement time the distribution becomes narrower. We see that the statistics of time averages clearly depend on the interpretation.

## III. BOUNDED PROCESSES

In the previous sections we have studied processes in an infinite domain. In many examples, ergodicity is discussed in the context of a finite sized system, simply because thermodynamics is valid for systems of finite (though large) size. Hence, we wish to explore infinite ergodic theory for inhomogeneous diffusion in a finite domain. In previous section, the infinite size system limited us to the condition of  $\alpha > 0$ . Here, we examine bounded processes, namely when  $x \in [0, L]$ . This allows us to choose negative  $\alpha$ , provided the growth condition holds, see [4] and App. A. As will be shown in the following, the non-integrable point of the zero-current solution  $\mathcal{I}_{\infty}(x)$  is at  $x \rightarrow 0$  (instead of  $x \rightarrow \infty$  as in the positive  $\alpha$  cases above).

### A. Pure Power-law dependent $\sqrt{D(x)}$ with Stratonovich Interpretation

For simplicity here we consider only the Stratonovich interpretation. The process is bounded in  $[0, L]$  and

$$\sqrt{D(x)} = \sqrt{2D_0}|\alpha|(x/\ell)^{1-1/\alpha} \text{ when } 0 \leq x \leq L \quad (38)$$



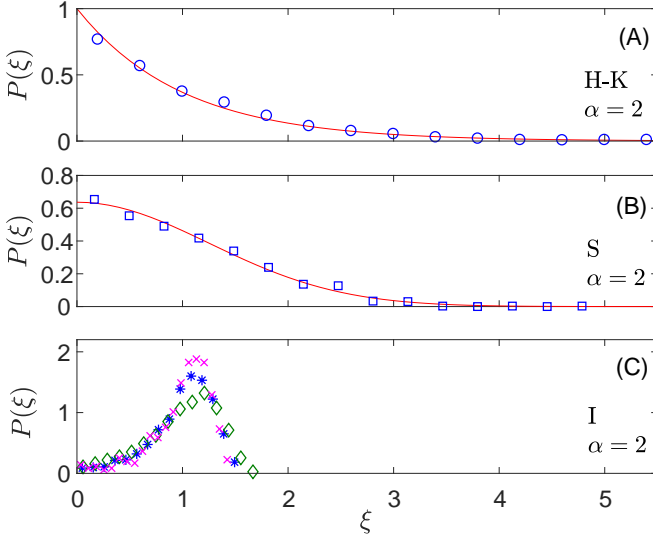


FIG. 6: The PDF  $P(\xi)$  for  $\xi$  defined in Eq. (24) with  $\mathcal{O}[x(t)] = \theta(|x(t)| < 10)$ . Here  $\sqrt{D(x)}$  is given in Eq. (28) with  $\alpha = 2$ . The data is from  $10^4$  realizations. Notice that all panels share the same x-axis. The symbols represent the data from simulations: Hänggi-Klimontovich (panel (A),  $t = 10^5$ , blue circles), Stratonovich [panel (B),  $t = 10^5$ , blue rectangles], and Itô [panel (C),  $t = 10^3$  (green diamonds),  $t = 10^5$  (blue stars),  $t = 10^6$  (pink crosses)]. In panels (A) and (B) we also compare simulations with the analytic predictions given in Eq. (37) (red solid curves). For the Itô interpretation, shown in panel (C),  $P(\xi)$  approaches a delta function in the long time limit.

with  $\alpha < 0$ . Clearly as  $x \rightarrow 0$  the diffusivity becomes small, and hence intuitively a particle in the vicinity of zero is slowed down. This, in turn, implies a pile up of particles close to zero, which is associated with the non-integrable state. Then the infinite density which, as mentioned, is defined via Eq. (13), is

$$\mathcal{I}_\infty(x) = CD(x)^{-1/2} = C \frac{\ell^{1-1/\alpha}}{\sqrt{2D_0\alpha^2}} x^{-1+1/\alpha}, \quad (39)$$

where  $C$  is determined below using the time-dependent solution. Here  $\mathcal{I}_\infty(x)$  is nonnormalizable due to its behavior close to zero.

To solve the Fokker-Planck equation (5), we define a new variable

$$y(x) \equiv \int_x^L \frac{dx'}{\sqrt{D(x')}} = \frac{\ell^{1-1/\alpha}}{\sqrt{2D_0}} \left[ x^{1/\alpha} - L^{1/\alpha} \right], \quad (40)$$

then Eq. (5), with  $A = 1$  (i.e. Stratonovich form), transforms into

$$\frac{\partial}{\partial t} P(y, t) = \frac{1}{2} \frac{\partial^2}{\partial y^2} P(y, t) \quad (41)$$

in the interval  $y \in [0, \infty)$  with the reflecting boundary condition  $\partial_y P(y, t)|_{y=0} = 0$ . Solving Eq. (41) with the method of images, considering the initial condition

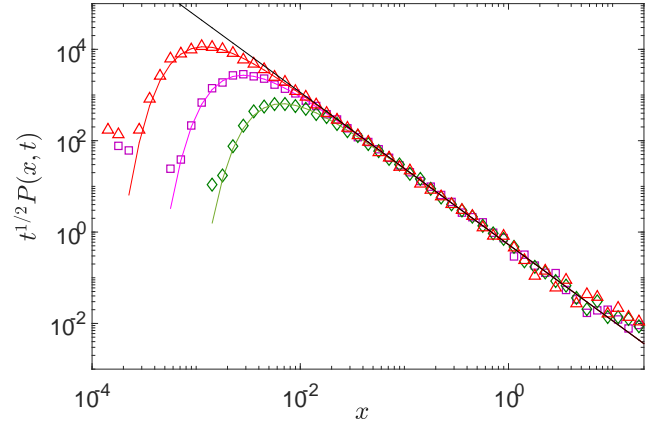


FIG. 7: The scaled PDF  $t^{1/2}P(x, t)$  for the process with diffusivity Eq. (38),  $\alpha = -1.5$ ,  $L = 20$ , and times  $t = 316$  (green diamonds),  $t = 1000$  (pink squares) and  $t = 3162$  (red triangle). The coloured solid curves are Eq. (42). The collapse for large  $x$  of data to the infinite density [black line, Eq. (43)] is clearly visible. The number of particles is  $10^4$ , and the Stratonovich interpretation is considered.

$y(t)|_{t=0} = y_0$ , and transforming back to  $x$  using Eq. (40), gives

$$P(x, t) = \frac{(x/\ell)^{-1+1/\alpha}}{\sqrt{4D_0\pi t}|\alpha|} \left\{ \exp \left[ -\frac{\left(x^{\frac{1}{\alpha}} - x_0^{\frac{1}{\alpha}}\right)^2 \ell^{2-\frac{2}{\alpha}}}{4D_0 t} \right] + \exp \left[ -\frac{\left(x^{\frac{1}{\alpha}} + x_0^{\frac{1}{\alpha}} - 2L^{\frac{1}{\alpha}}\right)^2 \ell^{2-\frac{2}{\alpha}}}{4D_0 t} \right] \right\}. \quad (42)$$

The following relation between the time-dependent solution  $P(x, t)$  and the infinite density in Eq. (39) is fulfilled

$$\lim_{t \rightarrow \infty} t^{1/2} P(x, t) = \sqrt{\frac{1}{\pi D_0 \alpha^2}} (x/\ell)^{-1+1/\alpha} = \mathcal{I}_\infty(x), \quad (43)$$

hence we identify the constant to be  $C = (2\pi)^{-1/2}$ .

In Fig. 7 we present  $t^{1/2}P(x, t)$  versus  $x$  for several times. The symbols are the simulation results and the solid curves represent the analytic prediction. The collapse of the data for large  $x$  and the approach to  $\mathcal{I}_\infty(x)$  while increasing the time are clearly visible.

### 1. Infinite Ergodic Theorem

Consider the observable  $\mathcal{O}[x(t)] = x^2(t)$ . This observable is integrable with respect to the infinite density Eq. (43) when  $\alpha < -1/2$ . Thus  $x^2(t)$ , when plotted versus time, exhibits long sojourn times close to zero, see



the illustration in Fig. 8. The ensemble average of  $x^2$  is

$$\begin{aligned}\langle x^2 \rangle &\stackrel{t \rightarrow \infty}{\approx} t^{-1/2} \int_0^L \sqrt{\frac{1}{\pi D_0 \alpha^2}} \frac{x^{1+1/\alpha}}{\ell^{-1+1/\alpha}} dx \\ &= t^{-1/2} \sqrt{\frac{1}{\pi D_0}} \frac{L^{2+1/\alpha}}{|2\alpha + 1| \ell^{-1+1/\alpha}}.\end{aligned}\quad (44)$$

In other words the ensemble average is computed with respect to the nonnormalized state  $\mathcal{I}_\infty(x)$ , which in that sense replaces the more typical invariant density of the system (when it exists).

For the simulations we use  $L = 20$  and  $\alpha = -3/2$ , hence  $t^{1/2} \langle x^2 \rangle \approx 21.658$ . The random variable  $\xi$  defined in Eq. (24) with  $\mathcal{O}[x(t)] = x^2(t)$ , using Eq. (25) with  $\beta = 1/2$ , is distributed according to

$$P(\xi) = \mathcal{M}_{1/2}(\xi) \equiv \frac{2}{\pi} \exp\left(-\frac{\xi^2}{\pi}\right),$$

i.e. the Mittag-Leffler function of order  $1/2$ , see

### B. Normal Diffusion Close to $x = L$ with Stratonovich Interpretation

In the previous example  $\mathcal{I}_\infty(x)$  decays as a power in the whole domain  $[0, L]$  peaking on  $x = 0$ . We consider

$$\begin{aligned}\sqrt{D(x)} &= \sqrt{2D_0} \left[ |\alpha| \left(\frac{x}{\ell}\right)^{1-1/\alpha} \theta(0 \leq x \leq x_c) + \theta(x_c < x \leq L) \right]\end{aligned}$$

where  $\alpha$  is negative.  $x_c$  is chosen so  $D(x)$  is continuous. Similar to the previous example,  $D(x)$  vanishes when  $x \rightarrow 0$ , but the field  $D(x)$  has some structure. Also here we define  $y(x) = \int_x^L dx' [D(x')]^{-1/2}$  and find the time dependent solution

$$\begin{aligned}P(x, t) &= \frac{1}{\sqrt{2\pi t D(x)}} \left\{ \exp\left[-\frac{(y(x) - y(x_0))^2}{2t}\right] \right. \\ &\quad \left. + \exp\left[-\frac{(y(x) + y(x_0))^2}{2t}\right] \right\}.\end{aligned}\quad (47)$$

The solution obtained from  $J = 0$ , see Eq. (13), is

$$\mathcal{I}_\infty(x) = \sqrt{\frac{1}{\pi D_0}} \begin{cases} \frac{1}{|\alpha|} \left(\frac{x}{\ell}\right)^{-1+1/\alpha} & 0 < x < x_c \\ 1 & x_c < x < L \end{cases} \quad (48)$$

which diverges due to its behavior in  $x = 0$ . Here,  $\lim_{t \rightarrow \infty} t^{1/2} P(x, t) = \mathcal{I}_\infty(x)$ . In Fig. 10 we show  $t^{1/2} P(x, t)$  versus  $x$  which approaches  $\mathcal{I}_\infty(x)$  as we increase  $t$ . Clearly, it illustrates that the structure of the infinite density  $\mathcal{I}_\infty(x)$  depends on  $D(x)$ .

Now we examine an observable which is integrable in respect to  $\mathcal{I}_\infty(x)$ , e.g. the mean-square-displacement

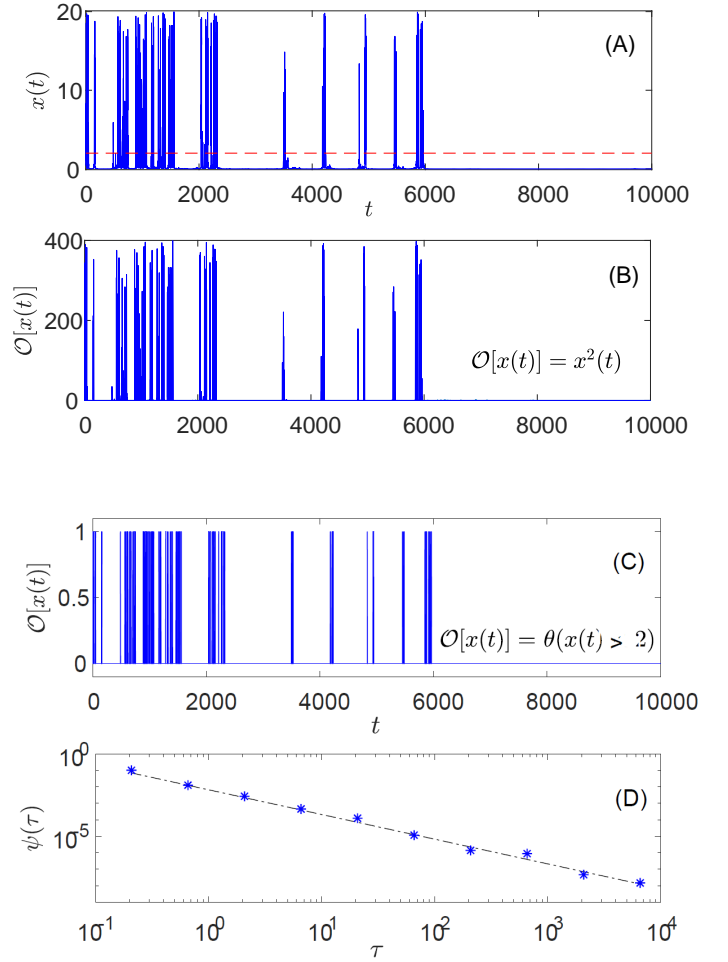


FIG. 8: Panel (A): A single realization  $x(t)$  where  $\sqrt{D(x)}$  is given in Eq. (38) with  $\alpha = -3/2$  and  $L = 20$ . The process is now bounded in  $[0, 20]$ , still infinite ergodic theory holds. A threshold on  $x = 2$  is represented with a red dashed line. Panels (B) and (C): The observable  $\mathcal{O}[x(t)] = x^2(t)$  and  $\mathcal{O}[x(t)] = \theta(x(t) > 2)$  respectively. Here,  $\theta(x(t) > 2) = 1$  if  $x(t) > 2$  and zero otherwise. The long sojourn times of  $\mathcal{O}[x(t)]$  close to zero is clearly visible. These are related to the slow-down of diffusion close to  $x \rightarrow 0$ . In Panel (D) we show the PDF  $\psi(\tau)$  of the sojourn times  $\tau$  of the trajectory  $x(t)$  below the threshold  $x = 2$ . The simulation results are given with blue stars. The black dashed line decreases as  $\propto \tau^{-3/2}$ , so  $\beta = 1/2$  in agreement with the analytic prediction, see III A 1 and Eq. (25).

(MSD)  $\mathcal{O}[x(t)] = x^2$  with  $\alpha < -1$ . Then the time-averaged MSD is controlled by the details of the non-

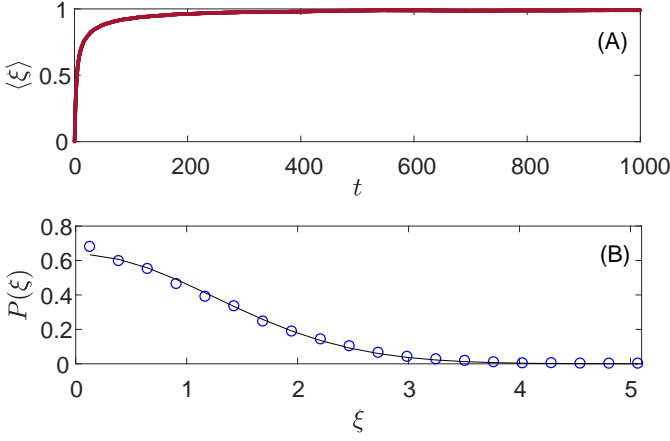


FIG. 9: Simulating the random variable  $\xi$  defined in Eq. (24) with the observable  $\mathcal{O}[x(t)] = x^2$  yield the average of  $\xi$  and its PDF. The diffusivity is given in Eq. (38), the measurement time is  $t = 10^3$ ,  $\alpha = -3/2$ ,  $L = 20$  and the number of particles is  $10^4$ . Panel (A) shows the convergence of  $\langle \xi \rangle$  to 1 when the time is long. Panel (B) presents the PDF of  $\xi$ . The simulation results are given with blue circles, and the analytic prediction Eq. (45) is the black line.

normalizable density  $\mathcal{I}_\infty(x)$ , since

$$\begin{aligned} \overline{\langle x^2(t) \rangle} &= \frac{1}{t} \int_0^t dt' \langle x^2(t') \rangle = \frac{1}{t} \int_0^t dt' \int_0^L dx P(x, t') x^2 \\ &\stackrel{t \rightarrow \infty}{\approx} \frac{1}{t} \int_0^t dt' \int_0^L dx (t')^{-\frac{1}{2}} \mathcal{I}_\infty(x) x^2 \\ &= \frac{t^{-\frac{1}{2}}}{1/2 \sqrt{\pi D_0}} \left[ \frac{\ell^{1-\frac{1}{\alpha}}}{(2+1/\alpha)|\alpha|} x_c^{2+\frac{1}{\alpha}} + \frac{L^3}{3} - \frac{x_c^3}{3} \right] \\ &= 2 \langle x^2 \rangle. \end{aligned} \quad (49)$$

From here, if  $\alpha = -3/2$  so  $x_c \approx 0.784$ , and  $L = 10$  we get  $t^{1/2} \langle x^2 \rangle \approx 266.12$ , which is used in Fig. 11 [panel (A)]. We define a variable  $\xi \equiv \overline{x^2(t)} / [2 \langle x^2(t) \rangle]$ , similar to Eq. (24) with  $\beta = 1/2$ , so  $\lim_{t \rightarrow \infty} \langle \xi \rangle = 1$ , and its PDF  $P(\xi)$  follows Eq. (36). Fig. 11 presents (with red stars) the simulation results for  $\langle \xi \rangle$  [panel (A)] and  $P(\xi)$  [panel (C)] with  $\alpha = -3/2$ . The measurement time is  $t = 10^3$  and the ensemble size is  $10^4$  particles. The agreement with infinite ergodic theory is visible.

#### IV. POWER-LAW BEHAVIOR CLOSE TO MORE THAN ONE POINT

In the previous sections we have shown that when the diffusion coefficient has the form Eq. (3) we find a nonnormalizable steady state and infinite ergodic theory holds. These results, for negative  $\alpha$ , are related to the fact that the spatially dependent diffusion coefficient slows down the particles close to zero. Therefore, similar results are obtained when one chooses diffusion coefficients with more than one “pathological points” as is demonstrated in the following.

#### A. Example: Two divergent points

Consider a signal  $x(t)$  which evolves via the Langevin equation

$$\frac{dx}{dt} = \sqrt{2D_0} \cdot \frac{x}{L} \left(1 - \frac{x}{L}\right) \eta(t) \quad (50)$$

where the signal is bounded, i.e.  $0 \leq x(t) \leq L$ . We use Stratonovich approach and obtain that the time-dependent solution of the Fokker-Planck equation, with initial condition  $P(x, t)|_{t=0} = \delta(x - \frac{L}{2})$  and reflecting boundary condition

$$P(x, t) = \frac{L^2}{\sqrt{4D_0\pi tx(L-x)}} \exp \left[ -\frac{\ln^2 \left( \frac{x}{L-x} \right) L^2}{4D_0 t} \right], \quad (51)$$

which has the form of the log-normal distribution of the variable  $x/(L-x)$ . The zero-current solution  $\mathcal{I}_\infty(x)$ , which is obtain from Eq. (13), fulfills

$$\mathcal{I}_\infty(x) = \lim_{t \rightarrow \infty} t^{1/2} P(x, t) = \frac{L^2}{\sqrt{4D_0\pi x(L-x)}}, \quad (52)$$

which diverges due to the boundary points, i.e.  $x = 0$  and  $x = L$ . This result is demonstrated with simulations in Fig. 12. Notice that  $\mathcal{I}_\infty(x)$  is non-integrable at both  $x \rightarrow 0$  and  $x \rightarrow L$ .

Furthermore, we consider the observable  $\mathcal{O}(x(t)) = \theta(0.4 < x(t) < 0.6)$  which is integrable with respect to  $\mathcal{I}_\infty(x)$ . In Fig. 11 (blue circles) we show that for the variable  $\xi$ , see Eq. (24), we find  $\langle \xi \rangle \rightarrow 1$  in the long time limit [panel (B)]. We show that  $P(\xi)$  is the Mittag-Leffler distribution of order 1/2 Eq. (36) [panel (C)], as expected, using same arguments as given in previous sections, so the Aaronson-Darling-Kac theorem applies.

Above, we study observables that are integrable with respect to the infinite density, so the PDF of these observables' time average is the Mittag-Leffler distribution. Here, since we have two non-integrable points, the sojourn times PDFs of the path  $x(t)$  in  $(0.5, 1)$  and in  $(0, 0.5)$  are both power-law  $\psi(\tau) \sim \tau^{-3/2}$ . In this case, the distribution of some other observables which are non-integrable with respect to  $\mathcal{I}_\infty(x)$  are known as well. For example, in the long time limit, the occupation time in  $(0.5, 1)$  is distributed with the Lamperti distribution of order 1/2 which corresponds to the arcsine law, see [41, 44, 45].

#### V. DISCUSSION

Generally, the appearance of an infinite density with its peculiar non-integrable points is related to the classification of boundary points and to the interpretation of the Langevin equation [4, 39, 46]. The non-integrable point serve as a ‘natural’ boundary, which refers to a boundary

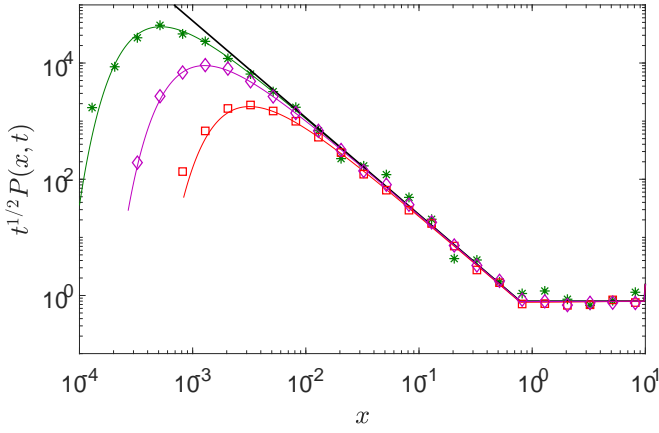


FIG. 10: The scaled PDF  $t^{1/2}P(x, t)$  for different times where  $\sqrt{D(x)} = |\alpha|x^{1-1/\alpha}\theta(0 \leq x \leq x_c) + \theta(x_c < x \leq L)$  with  $P(x, t)|_{t=0} = \delta(x - 1/2)$ . We use  $\alpha = -3/2$  and  $L = 10$ , hence  $x_c \approx 0.784$ . We present the simulation results for  $t = 10^3$  (red triangles),  $t = 3162$  (pink diamonds) and  $t = 10^4$  (green stars). The lines represent the analytic prediction Eq. (47) (with respect to the different times) and the black solid line is Eq. (48). The number of particles is 5000 (except for  $t = 10^4$  where  $10^3$  realizations were taken). Here the infinite density has a clear structure, beyond the simple power law presented in Fig. 7.

which can neither be reached in finite mean time nor be the starting point of a process.

For example, consider the process in  $[0, L]$  when  $\sqrt{D(x)} \sim x^{1-1/\alpha}$  where  $x \rightarrow 0$  with  $\alpha < 0$  (e.g. see Sec. III) with Stratonovich interpretation. There, the heterogeneous diffusion coefficient is effectively slowing the particle in a sufficient way, so the divergent point  $x \rightarrow 0$  actually serves as a 'natural' boundary since the particle never reaches the boundary, yet it approaches there slowly. Interestingly,  $\sqrt{D(x)} \sim x^{1-1/\alpha}$  vanishes when  $x \rightarrow 0$  for  $\alpha < 0$  or  $\alpha > 1$ , yet the infinite density appearance is related to the interpretation and the value of  $\alpha$  itself. For Itô and Stratonovich interpretations, we may find either an infinite density or a normalized one, within a finite domain, depends on  $\alpha$ . Hänggi-Klimontovich interpretation is significantly different, since thermal equilibrium is attained for every process defined in a finite domain with a valid diffusivity (i.e. when the growth condition is fulfilled). This is so since, from its construction the Hänggi-Klimontovich interpretation is built to yield a thermal state, which is a uniform distribution in a finite domain with reflecting boundary conditions and in the absence of external forces. In Table II we present for different diffusivities the different regimes depend in  $A$  and  $\alpha$ .

For unbounded processes, where  $\sqrt{D(x)} \sim x^{1-1/\alpha}$  for large  $x$  and  $\alpha > 0$  (see, e.g. Secs. II and IID), the zero-current solution  $\mathcal{I}_\infty(x)$  is non-integrable due its behavior at  $x \rightarrow \infty$ . In these cases  $D(x)$  does not necessarily vanish anywhere, and there are no particular points where

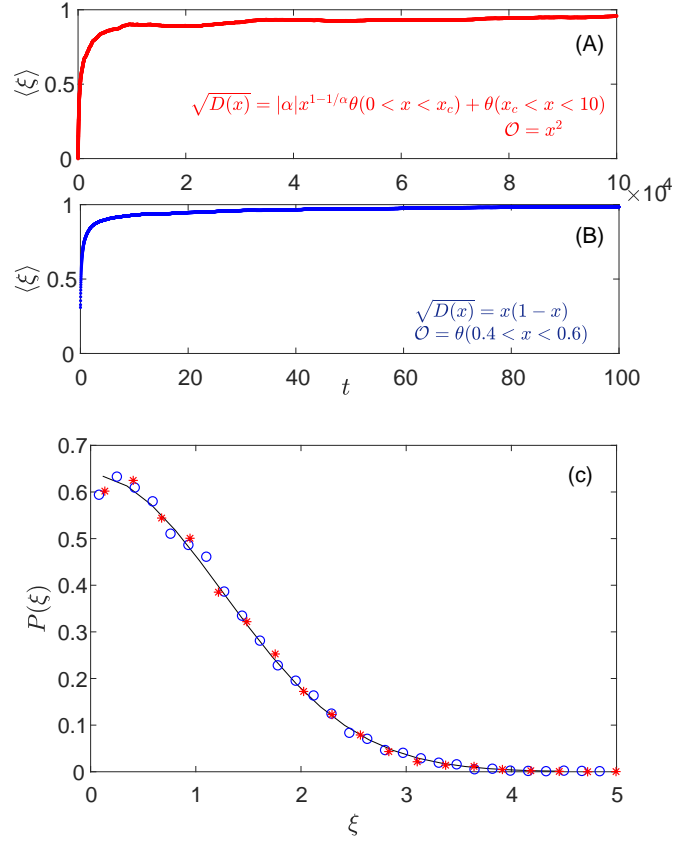


FIG. 11: Panels (A) and (B): The convergence of  $\langle \xi \rangle$  to 1, where  $\xi$  are defined in Eq. (24) with the observable  $\mathcal{O}[x(t)] = x^2(t)$  and the diffusivity given in Eq. (47) (panel (A), red) and  $\mathcal{O}[x(t)] = \theta(0.4 < x(t) < 0.6)$  for the process define in Eq. (50). (panel (B), blue). In (A) the measurement time is  $10^5$  and the number of particles is 600. In (B) the measurement time is  $10^2$  and 6000 realizations were used. Panel (C): The PDF of the random variables  $\xi$  which are defined in Eqs. (24) with  $\mathcal{O}[x(t)] = x^2(t)$  [red stars,  $t = 10^3, 10^5$  particles,  $\sqrt{D(x)} = |\alpha|x^{1-1/\alpha}\theta(0 \leq x \leq x_c) + \theta(x_c < x \leq L)$ ] and  $\mathcal{O}[x(t)] = \theta(0.4 < x(t) < 0.6)$  [blue circles,  $t = 10^2, 10^4$  particles,  $\sqrt{D(x)} = x(1-x)$ ]. The black curve represents the analytic prediction Eq. (36).

particles accumulate. Of-course, if the time-dependent distribution  $P(x, t)$  becomes broader with time, the point  $x \rightarrow \infty$  is a natural boundary. In Sec. IID the effective force with the Itô interpretation may limit the expansion of  $P(x, t)$ , so the equilibrium state is reached, see Tab II.

## VI. SUMMARY

We have shown that for processes with multiplicative noise, in particular diffusion in inhomogeneous space, infinite ergodic theory is the toolbox with which we analyze the long-time behavior of the system. We have shown that the appearance of an infinite density is not related to the entire structure of  $D(x)$  but it depends,

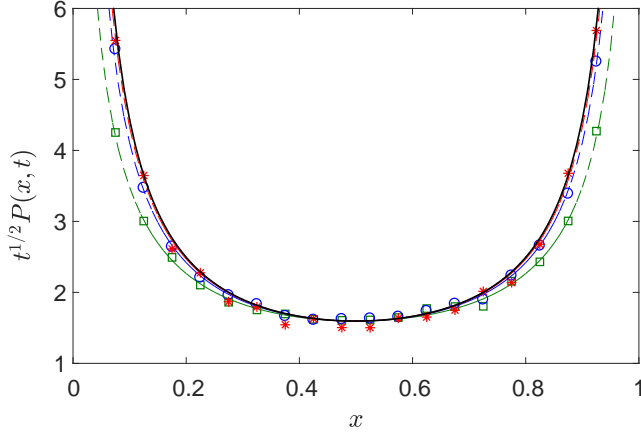


FIG. 12: The scaled PDF  $t^{1/2}P(x, t)$  for different times where  $\sqrt{D(x)} = x(1-x)$  with  $P(x, t)|_{t=0} = \delta(x - 1/2)$ . Here we present the simulation results for  $t = 10$  (green rectangles),  $t = 31$  (blue dots) and  $t = 100$  (red stars). The dashed lines represent the analytic prediction Eq. (51) (with respect to the different times) and the black solid line is Eq. (52). The number of particles is  $10^5$ .

together with the interpretation of the Langevin equation, on the behavior of  $D(x)$  at large  $x$  (for unbounded processes) or close to its zeros. In particular we study processes with  $D(x) \sim |x - \tilde{x}|^{2-2/\alpha}$  in the vicinity of a point  $\tilde{x}$ . We examined the PDF  $P(x, t)$  obtained from the Fokker-Planck equation corresponding to different interpretations of the Langevin equation; Itô, Stratonovich or Hänggi-Klimontovich. All these give rise to non-normalized densities,  $\mathcal{I}_\infty(x)$ , when the system is left un-

bounded, while Itô and Stratonovich interpretations yield a nonnormalized state even for a bounded process. In the long-time limit we find  $P(x, t) \rightarrow t^{\beta-1}\mathcal{I}_\infty(x)$ , where  $\beta$  is related to the first-passage-time distribution.

Furthermore, we consider observables  $\mathcal{O}[x(t)]$  which are integrable with respect to the infinite density and show that the PDF of  $\xi \equiv \lim_{t \rightarrow \infty} \beta \mathcal{O} / \langle \mathcal{O} \rangle$  follows Mittag-Leffler distribution of order  $\beta$  where  $\langle \xi \rangle = 1$ . This is in agreement with the Aaronson-Darling-Kac theorem. One of the main results here is the identification of the relations between the exponents describing the diffusion field  $D(x)$  and those describing the nonnormalized state and the Mittag-Leffler statistics. For that we find useful two transformations Eqs. (6) and (7) which map the problem to Bessel processes (with purely logarithmic potential) or regularized processes (where the potential is only asymptotically logarithmic in some regime), so we can get finite time solutions. In particular, for the former we get exact solutions for all times, which is of benefit since it explains how the system approaches the nonnormalized state and in what sense.

We note that all along our work we considered the time averages, which start at the moment of initiation of the process. That in a diffusion process corresponds to a medium, in which a particle is inserted at some time which we call the origin of time. However, we may choose to start measuring at some time  $t_a$ , for example perform a time average in a window  $(t_a, t_a + t)$  and this would give aging effects. In deterministic setting the modification of the Aaronson-Darling-Kac theorem was considered in [47], and it might be worthy to consider this more general scenario in the context of theory of multiplicative processes.

## Acknowledgments

The support of Israel Science Foundation's grant 1898/17 is acknowledged. We thank Guenter Radons and Takuma Akimoto for the discussion and comments.

## Appendix A: Growth Condition

A mathematical issue arises when considering the process describe by Langevin equation (1) as is hereby explained. The following conditions guarantee the existence and uniqueness of the solution of the Langevin equation Eq. (1): a  $K \in \mathbb{R}^+$  exist such that for every time [4]

$$\begin{aligned} |\sqrt{D(x)} - \sqrt{D(y)}| &\leq K|x - y| \quad (\text{Lipschitz condition}), \\ D(x) &\leq K^2(1 + x^2) \quad (\text{growth condition}). \end{aligned}$$

These conditions should be satisfied for  $x$  and  $y$  in the underlined interval of a given process. Therefore the fol-

lowing requirements are taken:

$\sqrt{D(x)}$	Section	$\alpha$
pure power-law in $[0, \infty)$	II	$\alpha \geq 1$
regularized process in $(-\infty, \infty)$	IID	$\alpha > 0$
power-law behavior close to zero in $[0, L]$	III	$\alpha < 0$
		$\alpha \geq 1$

We note though that violation of the conditions does not necessarily mean that there is no solution, it rather means that the solution of Eq. (1) might diverge at finite time and thus does not describe a physical behavior. See further discussion in [4].

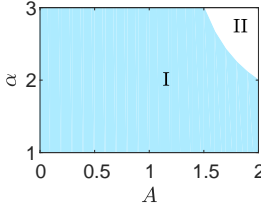
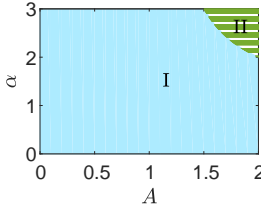
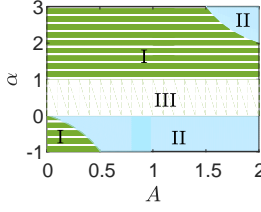
$\sqrt{D(x)}$	bounded/ unbounded	Sec.		
$\sqrt{D(x)} \propto x^{1-1/\alpha}$	unbounded	II		Region I - $\mathcal{I}_\infty(x)$ non-integrable, the non integrable point is $x \rightarrow \infty$ Region II - $P(x, t)$ non-exist
$\sqrt{D(x)} \propto x^{1-1/\alpha} \theta(x \geq x_c) + \theta(x < x_c)$	unbounded	IID		Region I - $\mathcal{I}_\infty(x)$ non-integrable, the non integrable point is $x \rightarrow \infty$ Region II - ergodic phase
$\sqrt{D(x)} \propto x^{1-1/\alpha} \theta(x_c < x < L) + \theta(x > x_c)$	bounded	III		Region I - ergodic phase Region II - $\mathcal{I}_\infty(x)$ non-integrable, the non integrable point is $x \rightarrow 0$ Region III - Growth condition is not fulfilled - processes are not defined

TABLE II: The different regimes, infinite density and ergodic phases, depend on  $\alpha$  and  $A$  for some diffusivities examine in the paper. Here  $A$  is considered a continuous parameter, though as was mentioned usually  $A = 0, 1, 2$  for I, S, and HK interpretations respectively. Only for convenience we limit the plots to  $\alpha < 3$ , though  $\alpha$  can attains values greater than 3. In the upper and the middle plots for values  $\alpha < 1$  and  $\alpha < 0$  (respectively) a solution  $P(x, t)$  does not exist. In the lower panel, there is no lower or upper bounds to  $\alpha$  and the choice of presenting  $-1 < \alpha < 3$  is arbitrary.

### Appendix B: Stratonovich Interpretation with external force approaches Hänggi-Klimontovich and Itô forms

Consider the following Fokker-Planck equation

$$\frac{\partial P(x, t)}{\partial t} = \frac{1}{2} \frac{\partial}{\partial x} \left[ D(x) \frac{\partial}{\partial x} P(x, t) \right], \quad (\text{B1})$$

which is related to the Langevin equation (1) with Hänggi-Klimontovich interpretation. This equation may also be written as

$$\begin{aligned} \frac{\partial P(x, t)}{\partial t} &= \frac{1}{2} \frac{\partial}{\partial x} \left[ D(x) \frac{\partial}{\partial x} P(x, t) \right] = \\ &= \frac{1}{2} \frac{\partial}{\partial x} \left[ \sqrt{D(x)} \frac{\partial}{\partial x} \sqrt{D(x)} P(x, t) \right] \\ &- \frac{1}{2} \frac{\partial}{\partial x} \left[ \sqrt{D(x)} \frac{\partial \sqrt{D(x)}}{\partial x} P(x, t) \right]. \quad (\text{B2}) \end{aligned}$$

Thus, the Stratonovich interpretation of a Langevin equation with an external potential is equivalent to the Langevin equation (1) with the Hänggi-Klimantovich ap-

proach. Its corresponding Langevin equation is

$$\frac{dx}{dt} = \sqrt{D(x)} \eta(t) + \frac{1}{2} \sqrt{D(x)} \frac{d\sqrt{D(x)}}{dx}. \quad (\text{B3})$$

Using the transformation  $y(x) = \int (D(x))^{-1/2} dx$  (which, as mentioned, may be applied just on Stratonovich interpretation) we find

$$\frac{dy}{dt} = \eta(t) + \frac{1}{2} \frac{d\sqrt{D(y)}}{dy} \frac{1}{\sqrt{D(y)}}. \quad (\text{B4})$$

The additional effective force, which is proportional to  $d_y \sqrt{D(y)} / \sqrt{D(y)}$ , is determined by the properties of  $\sqrt{D(y)}$ . Using Eq. (4) and we obtain

$$\frac{dy}{dt} = \eta(t) - \frac{(1 - \alpha)/2}{y} \quad (\text{B5})$$

which is a Brownian motion in a logarithmic potential as given in Eq. (8) with  $A = 0$ .

In a similar fashion the Fokker-Planck equation corre-

sponding Itô interpretation may be presented as

$$\begin{aligned}\frac{\partial P(x, t)}{\partial t} &= \frac{1}{2} \frac{\partial^2}{\partial x^2} [D(x)P(x, t)] = \\ &= \frac{1}{2} \frac{\partial}{\partial x} \left[ \sqrt{D(x)} \frac{\partial}{\partial x} \sqrt{D(x)}(x, t) \right] \\ &+ \frac{1}{2} \frac{\partial}{\partial x} \left[ \sqrt{D(x)} \frac{\partial \sqrt{D(x)}}{\partial x} P(x, t) \right], \quad (\text{B6})\end{aligned}$$

therefore

$$\frac{dy}{dt} = \eta(t) + \frac{(1 - \alpha)/2}{y}, \quad (\text{B7})$$

hence we recover Eq. (8) with  $A = 2$ .

### Appendix C: First Passage Time when $-1 < U_0 < 1$

Following [8], the distribution of  $y$  at time  $t$  with absorbing boundary at  $y = 0$  is

$$\tilde{P}_{\text{abs}}(y, t; y_0, 0) = e^{-\frac{y^2 + y_0^2}{2t}} y_0^{\frac{1}{2} + \frac{U_0}{2}} y^{\frac{1}{2} - \frac{U_0}{2}} I_{\frac{1}{2} + \frac{U_0}{2}} \left( \frac{y_0 y}{t} \right) \frac{1}{t}. \quad (\text{C1})$$

This solution exists (i.e. normalizable) when  $U_0 > -1$ . The current thus through the origin  $y = 0$  is

$$\begin{aligned}J(0) &\equiv -\frac{1}{2} \left[ \frac{\partial \tilde{P}_{\text{abs}}(y, t)}{\partial y} + \frac{U_0}{y} \tilde{P}_{\text{abs}}(y, t) \right]_{y=0} \\ &= \frac{2^{-\frac{U_0}{2} - \frac{1}{2}} t^{-\frac{U_0}{2} - \frac{3}{2}} \exp\left(-\frac{y_0^2}{2t}\right) y_0^{U_0+1}}{\Gamma\left[\frac{U_0}{2} + \frac{1}{2}\right]} \stackrel{t \rightarrow \infty}{\propto} t^{-\frac{U_0}{2} - \frac{3}{2}}\end{aligned} \quad (\text{C2})$$

which is a known result, see e.g. [8]. Back from  $y$  to  $x$  we find that the current of the probability at  $x = 0$  behaves the same, i.e.  $\propto t^{-(U_0+3)/2}$ . In a similar fashion one can prove that the probability of sojourn times  $\tau$  outside a finite subspace  $(x_1, x_2)$  follows

$$\psi(\tau) \sim \tau^{-1-\beta} \quad \text{with} \quad \beta = \frac{1 + U_0}{2}. \quad (\text{C3})$$

Using renewal processes theory [41] we find that  $\xi$  defined in Eq. (24) is distributed via PDF Eq. (27) as given in the main text.

### Appendix D: Derivation of the distribution of $\xi$

Consider a renewal process where the events occur at the random epoch, and the waiting times between the events distributed with

$$\psi(\tau) \sim \tau^{-1-\beta} \quad (\text{D1})$$

in the long time limit. The PDF of  $n$  renewals up to time  $t$  in Laplace space is

$$\mathcal{L}\{\text{PDF}[n]\} = \psi^n(s) \frac{1 - \psi(s)}{s}. \quad (\text{D2})$$

In the following we calculate this PDF for several cases of  $\psi(s)$ .

*Case 1: Infinite mean sojourn time, i.e.  $0 < \beta < 1$*

In this case, in the small  $s$  limit the the Laplace transform of Eq. (D1) reads

$$\psi(s) \sim 1 - \Gamma(1 - \beta) s^\beta + \dots \quad (\text{D3})$$

By substituting into Eq. (D2) we find

$$\mathcal{L}\{\text{PDF}[n]\} \approx e^{-\Gamma(1-\beta)ns^\beta} \Gamma(1 - \beta) s^{\beta-1}, \quad (\text{D4})$$

where the small  $s$  limit is taken. Its inverse Laplace transform gives

$$\text{PDF}[n] \approx \frac{t}{\beta n^{1+\frac{1}{\beta}} \Gamma(1 - \beta)^{\frac{1}{\beta}}} L_\beta \left[ \frac{t}{\Gamma(1 - \beta)^{\frac{1}{\beta}} n^{\frac{1}{\beta}}} \right]. \quad (\text{D5})$$

The mean of  $n$  is given by

$$\begin{aligned}\mathcal{L}[\langle n \rangle] &= \frac{\psi(s)}{s[1 - \psi(s)]} \approx \frac{s^{-\beta-1}}{\Gamma(1 - \beta)} \\ \Rightarrow \langle n(t) \rangle &\approx \frac{t^\beta}{\Gamma(1 - \beta)\Gamma(1 + \beta)}.\end{aligned} \quad (\text{D6})$$

Now, we define the scaling variable

$$\xi \equiv \frac{n}{\langle n \rangle} = \Gamma(1 - \beta)\Gamma(1 + \beta) \frac{n}{t^\beta}. \quad (\text{D7})$$

Therefore, the distribution of  $\xi$  is

$$P(\xi) = \mathcal{M}_\beta(\xi) \equiv \frac{\Gamma^{\frac{1}{\beta}}(1 + \beta)}{\beta \xi^{1+\frac{1}{\beta}}} L_\beta \left[ \frac{\Gamma^{\frac{1}{\beta}}(1 + \beta)}{\beta \xi^{\frac{1}{\beta}}} \right], \quad (\text{D8})$$

as is give in Eq. (27).

*Case 2: Finite mean sojourn time*

In this case, in the small  $s$  limit the the Laplace transform of Eq. (D1) reads

$$\psi(s) \sim 1 - \langle \tau \rangle s + \dots \quad (\text{D9})$$

By substituting into Eq. (D2) we find

$$\begin{aligned}\mathcal{L}\{\text{PDF}[n]\} &\approx e^{-n\langle \tau \rangle s} \langle \tau \rangle, \\ \rightarrow \text{PDF}[n] &\approx \langle \tau \rangle \delta(t - n\langle \tau \rangle),\end{aligned} \quad (\text{D10})$$

in the long time (small  $s$ ) limit. We define

$$\xi \equiv \frac{n}{\langle n \rangle} = \frac{n\langle \tau \rangle}{t}, \quad (\text{D11})$$

so

$$P(\xi) = \delta(\xi - 1). \quad (\text{D12})$$

In Sec. IID with Itô interpretation, a case where  $\beta > 1$  is possible, so the sojourn times' PDF has a mean. In these cases Eq. (D12) is obtained as is given in Eq. (37) for  $\beta \rightarrow 1$  (equivalent to  $\alpha \rightarrow 2$ ).

*Case 3: Limit of  $\beta \rightarrow 0$*

This case where  $\beta \rightarrow 0$ , is delicate since we should take both small  $s$  limit and the limit when  $\beta$  approaching to zero from above. Importantly, we first take the limit of small  $s$  and  $0 < \beta < 1$ , and then we calculate the limit when  $\beta \rightarrow 0$ . Using Eq. (D4) we obtain

$$\begin{aligned} \mathcal{L}\{\text{PDF}[n]\} &\approx e^{-\Gamma(1-\beta)ns^\beta} \Gamma(1-\beta)s^{\beta-1} \quad (\text{D13}) \\ &\Rightarrow \mathcal{L}\{\text{PDF}[n]\} \xrightarrow{\beta \rightarrow 0} \frac{1}{s} \exp(-n) \end{aligned}$$

and its inverse Laplace transform gives

$$\text{PDF}[n] = \mathcal{L}^{-1}\left[\frac{1}{s} \exp(-n)\right] = \exp(-n). \quad (\text{D14})$$

The rescaled variable is  $\xi \equiv n/\langle n \rangle = n$  (since  $\langle n \rangle = 1$ ) so

$$P(\xi) = \exp(-\xi) \quad (\text{D15})$$

as is given in Eq. (37) in the main text.

### Appendix E: Simulation Methods

There are mainly two methods to simulate Langevin equation with multiplicative noise regard to the different interpretations.

*Method 1:*

This method is based on the fact that for variable  $y$  [given from the mapping  $y(x)$ ] the process evolves with

additive noise instead of multiplicative noise. The algorithm is as follows

1. Transforming to variable  $y(t) \equiv y[x(t)]$  as given for example in Eq. (8) in the main text.

2. Using Euler discretization

$$y(t + \delta t) = y(y) + \eta \delta t - \frac{U_0/2}{y} \delta t. \quad (\text{E1})$$

3. Transforming back following  $x(t + \delta t) = y^{-1}(t + \delta t)$ .

*Method 2:*

Here, one can use the known transformations between the interpretations: Itô  $\leftrightarrow$  Stratonovich  $\leftrightarrow$  Hänggi-Klimontovich with addition of effective force. Since Euler discretization may be applied on Itô interpretation solely, we used the transformation from other interpretations to Itô and find

$$\dot{x}(t) = \sqrt{D(x)}\eta(t) + \frac{2-A}{2}\sqrt{D(x)}\frac{\partial\sqrt{D(x)}}{\partial x} \quad (\text{E2})$$

which is now interpret via Itô and we may use Euler discretization, i.e.

$$x(t + \delta t) = x(t) + \sqrt{D[x(t)]}\eta\delta t + \frac{2-A}{2}\sqrt{D(x)}\frac{\partial\sqrt{D(x)}}{\partial x}\delta t. \quad (\text{E3})$$

For both methods one should use small  $\delta t$ .

- 
- [1] P. Lançon, G. Batrouni, L. Lobry, and N. Ostrowsky, Euro. Phys. Lett. **54**, 28 (2001).
  - [2] J. Pešek, P. Baerts, B. Smeets, C. Maes, and H. Ramon, Soft matter **12**, 3360 (2016).
  - [3] S. Regev, N. Grønbech-Jensen, and O. Farago, Physical Review E **94**, 012116 (2016).
  - [4] C. W. Gardiner, *Handbook of Stochastic Methods for Physics, Chemistry and the Natural Sciences* (Springer, 2003).
  - [5] C. Cohen-Tannoudji, in *Fundamental Systems in Quantum Optics, Les Houches session LIII*, edited by J. Dalibard, J. M. Raimond, and J. Zinn-Justin (Elsevier Science, Amsterdam, 1992).
  - [6] F. Bardou, J.-P. Bouchaus, A. Aspect, and C. Cohen-Tannoudji, *Lévy statistics and laser cooling: how rare events bring atoms to rest* (Cambridge University Press, 2002).
  - [7] O. Farago and N. Grønbech-Jensen, The Journal of chemical physics **144**, 084102 (2016).
  - [8] A. Bray, Physical Review E **62**, 103 (2000).
  - [9] B. Oksendal, *Stochastic differential equations: an introduction with applications* (Springer Science & Business Media, 2013).
  - [10] S. Pieprzyk, D. Heyes, and A. Brańka, Biomicrofluidics **10**, 054118 (2016).
  - [11] A. M. Berezhkovskii and D. E. Makarov, The Journal of chemical physics **147**, 201102 (2017).
  - [12] T. Kühn, T. O. Ihalainen, J. Hyväluoma, N. Dross, S. F. Willman, J. Langowski, M. Vihinen-Ranta, and J. Timonen, PLoS One **6**, e22962 (2011).
  - [13] B. Kaulakys and M. Alaburda, J. Stat. Mech. Theo. Exp p. P02051 (2009).
  - [14] K. Itô, Proceedings of the Imperial Academy **20**, 519 (1944).
  - [15] R. Stratonovich, SIAM Journal on Control **4**, 362 (1966).
  - [16] P. Hanggi, Physical Review A **25**, 1130 (1982).
  - [17] Y. L. Klimontovich, Physica A: Statistical Mechanics and its Applications **163**, 515 (1990).
  - [18] R. Kubo, M. Toda, and N. Hashitsume, *Statistical physics II: nonequilibrium statistical mechanics* (Springer, 2012).
  - [19] E. Wong and M. Zakai, Ann. Math. Stat **36**, 1560 (1965).



- [20] G. Volpe and J. Wehr, Rep. Prog. Phys **79**, 053901 (2016).
- [21] J. Von Neumann, *Invariant measures* (American Mathematical Soc., 1991).
- [22] M. Thaler, Israel J. Math **46**, 67 (1983).
- [23] M. Thaler and R. Zweimüller, Probab. Theory Related Fields **135**, 15 (2006).
- [24] N. Korabel and E. Barkai, Phys. Rev. Lett. **102**, 050601 (2009).
- [25] T. Akimoto and T. Miyaguchi, Physical Review E **82**, 030102(R) (2010).
- [26] D. A. Kessler and E. Barkai, Phys. Rev. Lett **105**, 120602 (2010).
- [27] A. Rebenshtok, S. Denisov, P. Hänggi, and E. Barkai, Phys. Rev. E **90**, 062135 (2014).
- [28] E. Aghion, D. A. Kessler, and E. Barkai, arXiv preprint arXiv:1804.05571 (2018).
- [29] J. Aaronson, *An introduction to infinite ergodic theory*, 50 (American Mathematical Soc., 1997).
- [30] J. Aaronson, M. Thaler, and R. Zweimüller, Ergodic Theory and Dynamical Systems **25**, 959 (2005).
- [31] L. F. Richardson, Proc. R. Soc. Lond. A **110**, 709 (1926).
- [32] G. Biroli, G. Bunin, and C. Cammarota, arXiv preprint arXiv:1710.03606 (2017).
- [33] A. G. Cherstvy, A. V. Chechkin, and R. Metzler, New J. Phys. **15**, 083039 (2013).
- [34] A. G. Cherstvy and R. Metzler, Phys. Chem. Chem. Phys. **15**, 20220 (2013).
- [35] A. G. Cherstvy and R. Metzler, Phys. Rev. E **90**, 012134 (2014).
- [36] A. G. Cherstvy and R. Metzler, J. Stat. Mech: Theo. Exp. **2015**, P05010 (2015).
- [37] B. O'Shaughnessy and I. Procaccia, Physical Review Letters **54**, 455 (1985).
- [38] S. Havlin and D. Ben-Avraham, Advances in Physics **36**, 695 (1987).
- [39] E. Martin, U. Behn, and G. Germano, Physical Review E **83**, 051115 (2011).
- [40] S. Redner, *A guide to first-passage processes* (Cambridge University Press, 2001).
- [41] C. Godreche and J. Luck, J. Stat. Phys. **104**, 489 (2001).
- [42] R. Metzler, J.-H. Jeon, A. G. Cherstvy, and E. Barkai, Physical Chemistry Chemical Physics **16**, 24128 (2014).
- [43] A. Dechant, E. Lutz, E. Barkai, and D. Kessler, Journal of Statistical Physics **145**, 1524 (2011).
- [44] G. Margolin and E. Barkai, J. Stat. Phys. **122**, 137 (2006).
- [45] T. Akimoto, Journal of Statistical Physics **132**, 171 (2008).
- [46] W. Feller, *An Introduction to Probability Theory and Its Applications* (1965).
- [47] T. Akimoto and E. Barkai, Phys. Rev. E **87**, 032915 (2013).